



|  |                           |                         |
|--|---------------------------|-------------------------|
| <i>Title:</i> NEON Algorithm Theoretical Basis Document – Frequency Response Corrections | <i>Author:</i> S. Metzger | <i>Date:</i> 08/02/2013 |
| NEON.DOC.000854  |                           | <i>Revision:</i> A      |

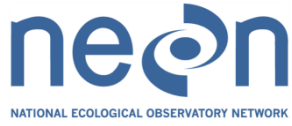
## NEON ALGORITHM THEORETICAL BASIS DOCUMENT: FREQUENCY RESPONSE CORRECTIONS FOR THE EDDY-COVARIANCE TURBULENT EXCHANGE SUBASSEMBLY

| PREPARED BY    | ORGANIZATION | DATE       |
|----------------|--------------|------------|
| Stefan Metzger | FIU          | 05/09/2013 |
|                |              |            |

| APPROVALS (Name) | ORGANIZATION | APPROVAL DATE |
|------------------|--------------|---------------|
| Hanne Buur       | CCB DIR SE   | 08/02/2103    |
| David Tazik      | CCB PROJ SCI | 06/04/2013    |
|                  |              |               |
|                  |              |               |

| RELEASED BY (Name) | ORGANIZATION | RELEASE DATE |
|--------------------|--------------|--------------|
| Stephen Craft      | SE           | 08/02/2013   |

See Configuration Management System for approval history.



|  |                           |                         |
|--|---------------------------|-------------------------|
| <i>Title:</i> NEON Algorithm Theoretical Basis Document – Frequency Response Corrections | <i>Author:</i> S. Metzger | <i>Date:</i> 08/02/2013 |
| NEON.DOC.000854  |                           | <i>Revision:</i> A      |

### CHANGE RECORD

| REVISION | DATE       | ECO #     | DESCRIPTION OF CHANGE |
|----------|------------|-----------|-----------------------|
| A        | 08/02/2013 | ECO-01053 | Initial Release       |
|          |            |           |                       |

|   |                           |                         |
|---|---------------------------|-------------------------|
| <i>Title:</i> NEON Algorithm Theoretical Basis Document –<br>Frequency Response Corrections | <i>Author:</i> S. Metzger | <i>Date:</i> 08/02/2013 |
| NEON.DOC.000854   |                           | <i>Revision:</i> A      |

## TABLE OF CONTENTS

|       |  |    |
|-------|--|----|
| 1     | DESCRIPTION.....                                     | 1  |
| 1.1   | Purpose .....  | 1  |
| 1.2   | Scope.....   | 1  |
| 2     | RELATED DOCUMENTS.....                               | 1  |
| 2.1   | Applicable documents .....                           | 1  |
| 2.2   | Reference documents.....                             | 2  |
| 2.3   | Verb convention.....                                 | 2  |
| 3     | DESCRIPTION OF VARIABLES.....                        | 2  |
| 3.1   | Reported variables.....                              | 3  |
| 3.2   | Input variables .....                                | 3  |
| 3.3   | Product instances.....                               | 4  |
| 3.4   | Temporal resolution and extent .....                 | 4  |
| 3.5   | Spatial resolution and extent.....                   | 4  |
| 4     | SCIENTIFIC CONTEXT .....                             | 4  |
| 4.1   | Theory of measurement/observation .....              | 4  |
| 4.2   | Theory of algorithm .....                            | 5  |
| 4.2.1 | Wavelet-based spectral correction method .....       | 8  |
| 4.2.2 | Discrete wavelet transform.....                      | 9  |
| 4.2.3 | Spectral peaks .....                                 | 11 |
| 4.2.4 | Power law coefficient in the inertial subrange ..... | 11 |
| 4.2.5 | Distribution of amplitude adjustment .....           | 12 |
| 4.2.6 | Correction for high-frequency loss .....             | 12 |

|   |                           |                         |
|---|---------------------------|-------------------------|
| <i>Title:</i> NEON Algorithm Theoretical Basis Document –<br>Frequency Response Corrections | <i>Author:</i> S. Metzger | <i>Date:</i> 08/02/2013 |
| NEON.DOC.000854   |                           | <i>Revision:</i> A      |

|       |   |    |
|-------|---|----|
| 4.2.7 | Reconstruction of the corrected time series ..... | 13 |
| 5     | ALGORITHM IMPLEMENTATION .....                    | 13 |
| 6     | UNCERTAINTY .....                                 | 13 |
| 6.1   | Analysis of uncertainty.....                      | 14 |
| 6.2   | Reported uncertainty.....                         | 14 |
| 7     | ALGORITHM VERIFICATION.....                       | 14 |
| 8     | SCIENTIFIC AND EDUCATIONAL APPLICATIONS .....     | 15 |
| 9     | FUTURE PLANS AND MODIFICATIONS .....              | 15 |
| 10    | APPENDIX .....                                    | 15 |
| 10.1  | Acronyms.....                                     | 15 |
| 10.2  | Functions .....                                   | 16 |
| 10.3  | Parameters .....                                  | 17 |
| 10.4  | Subscripts .....                                  | 17 |
| 10.5  | Variables.....                                    | 18 |
| 11    | BIBLIOGRAPHY .....                                | 19 |

## LIST OF TABLES AND FIGURES

|                  |  |    |
|------------------|--|----|
| <b>Figure 1.</b> | Normalized power spectrum for an ideal instrument which measures the unaffected spectrum of turbulence, and for a non-ideal instrument. .... | 6  |
| <b>Figure 2.</b> | Overview of the wavelet-based spectral correction method for four case studies.....  | 9  |
| <b>Figure 3.</b> | Relation of the resolution of location and scale for the discrete wavelet transform .....  | 10 |
| <b>Table 1.</b>  | List of variables that are produced in this ATBD.....  | 3  |
| <b>Table 2.</b>  | List of input variables that are used in this ATBD. ....   | 3  |

|   |                           |                         |
|---|---------------------------|-------------------------|
| <i>Title:</i> NEON Algorithm Theoretical Basis Document –<br>Frequency Response Corrections | <i>Author:</i> S. Metzger | <i>Date:</i> 08/02/2013 |
| NEON.DOC.000854   |                           | <i>Revision:</i> A      |

## 1 DESCRIPTION

NEON shall measure the exchange of momentum, energy and trace gases between the earth’s surface and the atmosphere. To accomplish this, NEON will operate an eddy covariance turbulent exchange subsystem (EC-TES, a summary of all acronyms, functions, parameters and variables is provided in Sect. 10), which collectively embodies a suite of sensors.

### 1.1 Purpose

This document describes the theoretical background and entire algorithmic process for correcting the limited high-frequency response of outputs from EC-TES sensors. The present algorithm theoretical basis document (ATBD) serves to summarize all corresponding algorithms which will be used during the implementation of AD[01].

### 1.2 Scope

This ATBD is embedded in a suite of 29 existing and upcoming NEON documents, which collectively describe the acquisition, processing and quality control of data from the EC-TES (AD[01] provides an overview). As such, the scope of this ATBD is to provide all necessary processing steps between immediately preceding and succeeding documents. This ATBD first introduces related documents, acronyms and conventions (Sect. 2). Throughout Sects. 3–6, (i) all reported variables and input variables are identified, (ii) theoretical background is provided, (iii) explicit algorithm descriptions are given, and (iv) error propagation algorithms are provided that enable the calculation of uncertainty budgets for each reported variable. This document does not provide computational implementation details, except for cases where these stem directly from algorithmic choices explained here.

## 2 RELATED DOCUMENTS

### 2.1 Applicable documents

|        |  |
|--------|--|
| AD[01] | NEON.DOC.000573    FIU Plan for airshed QA/QC development                      |
| AD[02] | NEON.DOC.000853    Coordinate rotations ATBD                                   |
| AD[03] | NEON.DOC.000823    Calculation of variances and covariances ATBD               |
| AD[04] | NEON.DOC.000465    Eddy-covariance turbulent exchange subsystem C <sup>3</sup> |
| AD[05] | NEON.DOC.000651    Atmospheric properties/units ATBD                           |

|   |                    |                  |
|---|--------------------|------------------|
| Title: NEON Algorithm Theoretical Basis Document – Frequency Response Corrections | Author: S. Metzger | Date: 08/02/2013 |
| NEON.DOC.000854   |                    | Revision: A      |

|        |  |  |
|--------|--|--|
| AD[06] | NEON.DOC.000822  | Eddy-Covariance Storage Exchange ATBD          |
| AD[07] | NEON.DOC.001097  | FFT/Wavelet Analysis/Spectral ATBD             |
| AD[08] | <a href="#">Freely available source code</a> to Nordbo, A. & Katul, G. (2012) A wavelet-based correction method for eddy-covariance high-frequency losses in scalar concentration measurements. <i>Boundary-Layer Meteorology</i> , <b>146</b> , 81-102. |  |
| AD[09] | NEON.DOC.000848  | NEON Science Commissioning and Validation Plan |

## 2.2 Reference documents

|        |                 |                        |
|--------|-----------------|------------------------|
| RD[01] | NEON.DOC.000008 | NEON Acronym List      |
| RD[02] | NEON.DOC.000243 | NEON Glossary of Terms |

## 2.3 Verb convention

"Shall" is used whenever a specification expresses a provision that is binding. The verbs "should" and "may" express non-mandatory provisions. "Will" is used to express a declaration of purpose on the part of the design activity.

## 3 DESCRIPTION OF VARIABLES

The algorithms in this ATBD provide all necessary processing steps between immediately preceding and succeeding ATBDs in a suite of NEON documents related to the EC-TES (Sect. 1.2, AD[01]). In general, the input variables of this ATBD are generated in preceding EC-TES-related documents, and the reported variables are used in succeeding documents. Which of these variables will be mapped to NEON data products (DP), as well as their corresponding IDs will be defined in succeeding documents, and are not provided in this ATBD.

### 3.1 Reported variables

Table 1 details the variables reported by the algorithms disclosed in this ATBD.

Table 1. List of variables that are produced in this ATBD.

| Variable  | Units               |
|---|---------------------|
| Time series (0.05 s temporal resolution) of atmospheric scalar, corrected for high-frequency loss ( $X_c$ )   | Depending on scalar |
| One quality metric for $X$ per averaging period, indicating whether high-frequency loss correction could be performed ( $QM_{att} = 0\%$ ) or not ( $QM_{att} = 100\%$ ). | %                   |

### 3.2 Input variables

Table 2 lists all input variables that are used to produce the output variables reported above. The data sources and specific data product IDs will be provided in ATBDs that use the variables listed in Table 2.

Table 2. List of input variables that are used in this ATBD.

| DP  | Units                     |
|---|---------------------------|
| <b>Ultrasonic anemometer variables</b>  |                           |
| Time series (0.05 s temporal resolution) of the vertical wind component, perpendicular to mean streamline ( $w$ , AD[02])   | $m\ s^{-1}$               |
| <b>Infrared gas analyzer variables</b>  |                           |
| Time series (0.05 s temporal resolution) of atmospheric scalar ( $X$ )  | Depending on scalar       |
| <b>Auxiliary variables</b>  |                           |
| Synchronization time lag ( $l_x$ )  | s                         |
| Individually for $w$ and $X$ , hard quality flag time series (0.05 s temporal resolution), indicating suitable ( $QF_{hard} = 0$ ) or unsuitable ( $QF_{hard} = 1$ ) measurement conditions (AD[03]). | Dimensionless<br>(0 or 1) |
| Individually for $w$ and $X$ , one hard quality metric flag per averaging period, indicating suitable or unsuitable measurement conditions ( $QM_{hard}$ , AD[03]).                                   | %                         |

### 3.3 Product instances

Each NEON site with terrestrial infrastructure will produce an instance of the reported variables in Table 1.

### 3.4 Temporal resolution and extent

The temporal resolution of most reported variables in Table 1 is 0.05 s. Only the quality metric  $QM_{att}$  is reported only once per averaging period (0.5 h). The temporal extent of all reported variables is 0.5 h, i.e. the fundamental averaging period of DPs derived from the EC-TES. The temporal resolution of most input variables in Table 2 is 0.05 s. Only the quality metric  $QM_{hard}$  exists only once per averaging period (0.5 h). The temporal extent of all input variables is 0.5 h, i.e. a data set of 0.5 h duration shall be considered for each implementation of the presented algorithms.

### 3.5 Spatial resolution and extent

The input variables used in this ATBD are measured at a single position in space. Consequently both, input variables and reported variables are not spatially resolved. The spatial extent (path length) of all variables is  $\approx 10$  cm (AD[04]). The spatial representativeness of the variables reported in this ATBD is a function of several factors such as measurement height  $d_{z,m}$ , displacement height  $d_{z,d}$ , wind speed and direction, atmospheric stability and surface roughness (AD[05]). From dispersion modeling (e.g., Schmid, 1994, Vesala et al., 2008) it is found that  $10(d_{z,m} - d_{z,d}) \lesssim d_{x,FP90} \lesssim 100(d_{z,m} - d_{z,d})$ , where  $d_{x,FP90}$  is the cross-wind integrated upwind extent from within which 90% of a measured flux value is sourced. The spatial representativeness for each observation of the reported variables will be quantified in the relevant ATBD (AD[01] provides an overview).

## 4 SCIENTIFIC CONTEXT

The intention of NEON EC-TES measurements is to determine the surface-air exchange of momentum, heat, water vapor and  $CO_2$  from fast response measurements of the wind vector components, temperature, and scalar concentrations.

### 4.1 Theory of measurement/observation

The exchange of momentum, heat, water vapor,  $CO_2$  and other scalars between the earth's surface and the atmosphere is mainly governed by turbulent transport. Buoyancy as well as shear stress result in a turbulent wind field for most of the day (e.g., Stull, 1988). The eddy-covariance (EC) technique measures the properties of the turbulent wind field directly. This makes it the least invasive method currently available for direct and continuous observations of the surface-air exchange. The technique is based on the concept of mass conservation and makes use of the Reynolds decomposition (isolation of mean and fluctuating part) of relevant terms in the Navier-Stokes equation (e.g., Foken, 2008, Stull, 1988). With

several restrictions (AD[01]) the net flux  $F$  into or out of an ecosystem can be expressed as (e.g., Loescher et al., 2006);

$$\begin{aligned}
 F = & \int_0^{d_{z,m}} \frac{\partial \bar{X}}{\partial t} dz + \int_0^{d_{z,m}} \frac{\partial \overline{u'X'}}{\partial x} dz + \int_0^{d_{z,m}} \frac{\partial \overline{v'X'}}{\partial y} dz + \int_0^{d_{z,m}} \frac{\partial \overline{w'X'}}{\partial z} dz \\
 & \text{I} \qquad \qquad \qquad \text{II} \qquad \qquad \qquad \text{III} \qquad \qquad \qquad \text{IV} \\
 & + \int_0^{d_{z,m}} \frac{\partial \bar{u}\bar{X}}{\partial x} dz + \int_0^{d_{z,m}} \frac{\partial \bar{v}\bar{X}}{\partial y} dz + \int_0^{d_{z,m}} \frac{\partial \bar{w}\bar{X}}{\partial z} dz, \\
 & \qquad \qquad \qquad \text{V} \qquad \qquad \qquad \text{VI} \qquad \qquad \qquad \text{VII}
 \end{aligned} \tag{1}$$

with overbars denoting means, and primes denoting deviations from the mean. Here,  $X$  is a scalar quantity such as  $\text{H}_2\text{O}$  or  $\text{CO}_2$  mixing ratios;  $u$ ,  $v$  and  $w$  are along-, cross-, and vertical wind speeds with respect to the Cartesian coordinates  $x$ ,  $y$ , and  $z$ ;  $t$  is time, and  $d_{z,m}$  is the measurement height. Term I in Eq. (1) represents the positive or negative rate of change of  $X$  in the vertical column below the sensor, equivalent to storage. Terms II–IV represent the turbulent flux divergence, and terms V–VII represent advection through the layer between the surface and sensor. If the conditions at the measurement site fulfill several assumptions (details provided in AD[01]), terms I–III and V–VII cancel from Eq. (1), and term IV can be further simplified to;

$$F = \overline{w'X'}. \tag{2}$$

That is, in this case the net flux into or out of an ecosystem can be expressed as the covariance between the vertical wind and the scalar, which can be computed from EC-TES measurements alone. Whether or not this reduction of Eq. (1) is valid will be assessed in a series of tests during the implementation of AD[01]. Wherever possible, auxiliary measurements will be used to re-substitute non-negligible terms in Eq. (2), e.g. the storage term I (AD[06]).

## 4.2 Theory of algorithm

EC measurement systems, like all measuring instruments, act as filters, removing both high- and low-frequency components of a signal. High-frequency losses are mainly due to inadequate sensor frequency response, line averaging, sensor separation and, in closed-path infrared gas analyzer (IRGA) systems, air transport through a filter and a tube (Foken et al., 2012). Figure 1 schematically illustrates the impact of high frequency loss in the measurement of an atmospheric scalar  $X$ , such as  $\text{CO}_2$  or  $\text{H}_2\text{O}$  dry mole fraction, on spectral density (The calculation of power spectra are detailed in AD[07]). The frequency range of attenuation depends on the instrumental setup and especially the length and conditioning of the sample tube. It is often confined to frequencies beyond the spectral peak, which is referred to as the inertial subrange (ISR) of atmospheric turbulence. As can be seen from Eq. (2), high frequency losses in  $X$

propagate into the EC-TES flux measurement, and the corresponding cospectrum  $CO(w,X)$ . Low-frequency losses result from the finite sampling duration, with the averaging period not always being sufficiently long to include all relevant low frequencies. The subject of this ATBD is the correction of high-frequency losses, in order to avoid underestimating the variances and covariances of outputs from EC-TES sensors (up to 20%, Nordbo and Katul, 2012, AD[03]). Low-frequency losses are not subject of this ATBD, and will be addressed in a series of tests during the implementation of AD[01].

Until recently, two general approaches have been used to correct the effect of high-frequency attenuation of EC instruments on the measured fluxes. In the theoretical approach, the transfer function  $TF(w,X)$  is deduced from prior knowledge of the measuring system and a theoretical cospectral density function (e.g., Horst and Lenschow, 2009, Moore, 1986). In the experimental approach,  $TF(w,X)$  is calculated from the ratio of two simultaneously measured cospectra (e.g., Fratini et al., 2012, Runkle et al., 2012). In this approach one cospectrum refers to the filtered scalar of interest, and the other is considered as a reference and supposedly real cospectrum. In practice, the sensible heat cospectrum is usually used as reference (Foken et al., 2012).

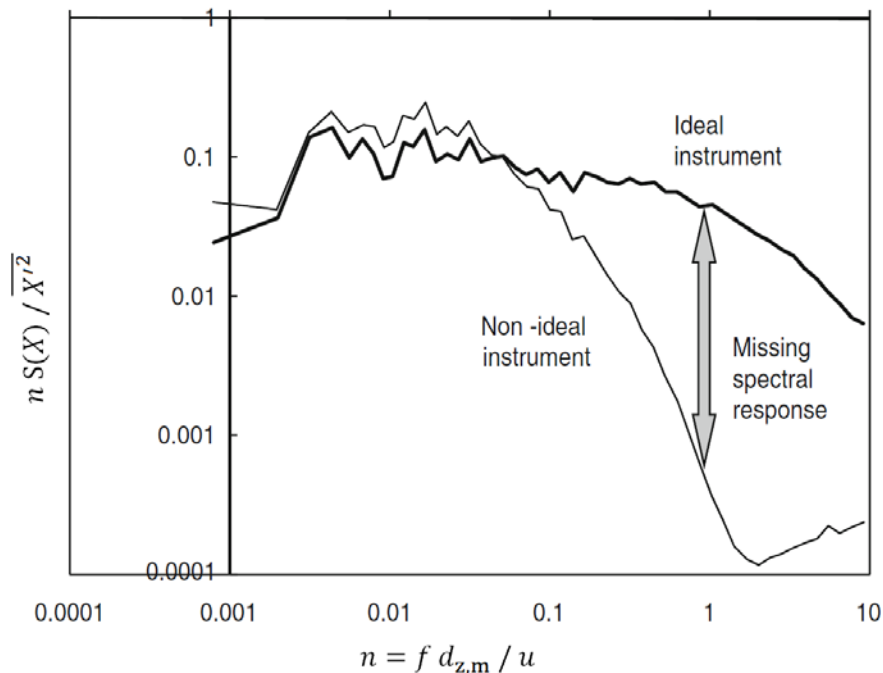


**Figure 1.** Modified after Foken et al. (2012): Normalized power spectrum for an ideal instrument which measures the unaffected spectrum of turbulence, and for a non-ideal instrument. The missing energy between both response curves must be corrected (normalized frequency  $n$ ; measurement frequency  $f$ , measurement height  $d_{z,m}$ , along-wind speed  $u$ , power spectrum and variance of atmospheric scalar  $X$ ,  $S(X)$  and  $\overline{X'^2}$ , respectively). The calculation of power spectra are detailed in AD[07].

|  |                           |                         |
|--|---------------------------|-------------------------|
| <i>Title:</i> NEON Algorithm Theoretical Basis Document – Frequency Response Corrections | <i>Author:</i> S. Metzger | <i>Date:</i> 08/02/2013 |
| NEON.DOC.000854  |                           | <i>Revision:</i> A      |

The theoretical approach has the advantage of relying on a fundamental description of the system and allows a comprehensive description of filtering processes. Its shortcomings are; (i) the theoretical cospectral densities not necessarily correspond to the real cospectral densities observed at the sites (e.g., De Ligne et al., 2010), (ii) a static transfer function cannot accommodate transient changes in a closed-path IRGA system, such as in the tube flow regime with ambient temperature, or in the adsorption/desorption behavior of the intake tube or the particle filter with accumulating dirt. While well suited for open-path IRGAs, the application of the theoretical approach to closed-path IRGA systems appears more difficult (Foken et al., 2012).

The experimental approach assumes that; (i) the high-frequency attenuation of sensible heat cospectral density is negligible compared with those affecting other tracers, and (ii) the processes of atmospheric turbulent transport of sensible heat and other tracers are similar and therefore the cospectral densities should be proportional to each other. The former assumption makes sense for closed-path systems where high-frequency losses are mainly resulting from tube or filter attenuation. In open-path systems however, the experimental approach could lead to an underestimation of the high-frequency correction (Foken et al., 2012). The second assumption, scalar similarity, generally holds true for the high-frequency part of the spectrum under daytime conditions. However, variations have been observed among scalars, as well as between different times of the day (Ruppert et al., 2006).

In order to combine the strengths of the theoretical and the empirical approaches, site-specific calibrations of the theoretical transfer functions have been derived (e.g., De Ligne et al., 2010, Spank and Bernhofer, 2008). Nevertheless, all of the forenamed approaches (i) are limited to correcting the resulting covariance Eq. (2) but do not restore the high-frequency data itself, and (ii) cannot easily be fully automated.

More recently Nordbo and Katul (2012, in the following referred to as NK12) have presented a novel approach to high frequency spectral corrections which (i) directly corrects the high-frequency data instead of the cospectrum, (ii) corrects each individual averaging period, and is thus able to take into account variations in environmental conditions (e.g., flow rate, relative humidity), (iii) does not assume cospectral similarity with heat, and (iv) does not rely on a theoretical shape for the velocity–scalar cospectrum, thereby making it advantageous to employ in non-ideal conditions. Furthermore, the method is not gas specific, and can be used with very little input information at various sites. The method’s largest insufficiency is its inability to correct attenuation starting already near the peak of power spectra, which however is explicitly taken into account in the design of NEON’s EC-TES. Consequently this is the method of choice for NEON, as it overcomes the drawbacks of the conventional approaches, and is fully automatable. Cospectral attenuation through sensor separation is not considered by the NK12 method. Instead it is explicitly addressed in AD[03] through maximization of the cross-correlation and by using an exponential decay model. Sect. 4.2.1 provides an overview of the NK12 method, including an outline of assumptions and idealizations. In Sects. 4.2.2–4.2.7 a detailed sequence of algorithmic steps is presented.

#### 4.2.1 Wavelet-based spectral correction method

The NK12 method uses the time-frequency localities of orthonormal wavelets to adjust high frequency time series prior to the computation of any turbulence statistics. It resembles a transfer-function method, because lost variance is recreated using a power spectral model. However, instead of only correcting variance loss, the procedure in the wavelet half-plane also enables correcting travel time distortions, e.g. resulting from tube wall effects. The NK12 method poses the following assumptions;

- (i) The peak of  $S(w)$  occurs at frequencies that are higher than the peak of  $S(X)$ ;
- (ii) The variance loss in  $X$  occurs at frequencies that are higher than the peak frequency of  $S(w)$ ;
- (iii)  $S(X)$  possesses a power-law decay in the ISR.

These assumptions are relatively weak compared to those of the conventional approaches. Moreover, assumption (ii) can be taken into consideration in the design process of an EC system, and assumptions (i) and (iii) are supported by experimental findings under a broad variety of environmental conditions (Kaimal and Finnigan, 1994 provide a comprehensive summary). Figure 2 gives an overview of the NK12 spectral correction method consisting of the following subsequent steps;

- (i) In Sect. 4.2.2 a discrete wavelet transform is performed on  $w$  and  $X$ , and their wavelet power spectra are determined;
- (ii) In Sect. 4.2.3 the spectral peak  $n_{\max}$  of the  $w$  power spectrum is determined. It is preconditioned that the scalar power spectrum  $S(X)$  is not attenuated for frequencies  $n(S(X)) \leq n_{\max}(S(w))$ , and spectral correction is only required for frequencies  $n(S(X)) > n_{\max}(S(w))$ ;
- (iii) In Sect. 4.2.4 the slope of the power-law decay in the ISR is determined from regression over  $S(X)$  in the frequency range that falls within the ISR and fulfills the condition  $n(S(X)) \leq n_{\max}(S(w))$ . For each frequency in the range  $n(S(X)) > n_{\max}(S(w))$  the required amplitude adjustment for  $S(X)$  is determined as the difference of the extrapolated power-law slope and  $S(X)$ ;
- (iv) In Sect. 4.2.5 only those wavelet coefficients of  $X$  are selected which coincide with high energy in the wavelet coefficients of  $w$ ;

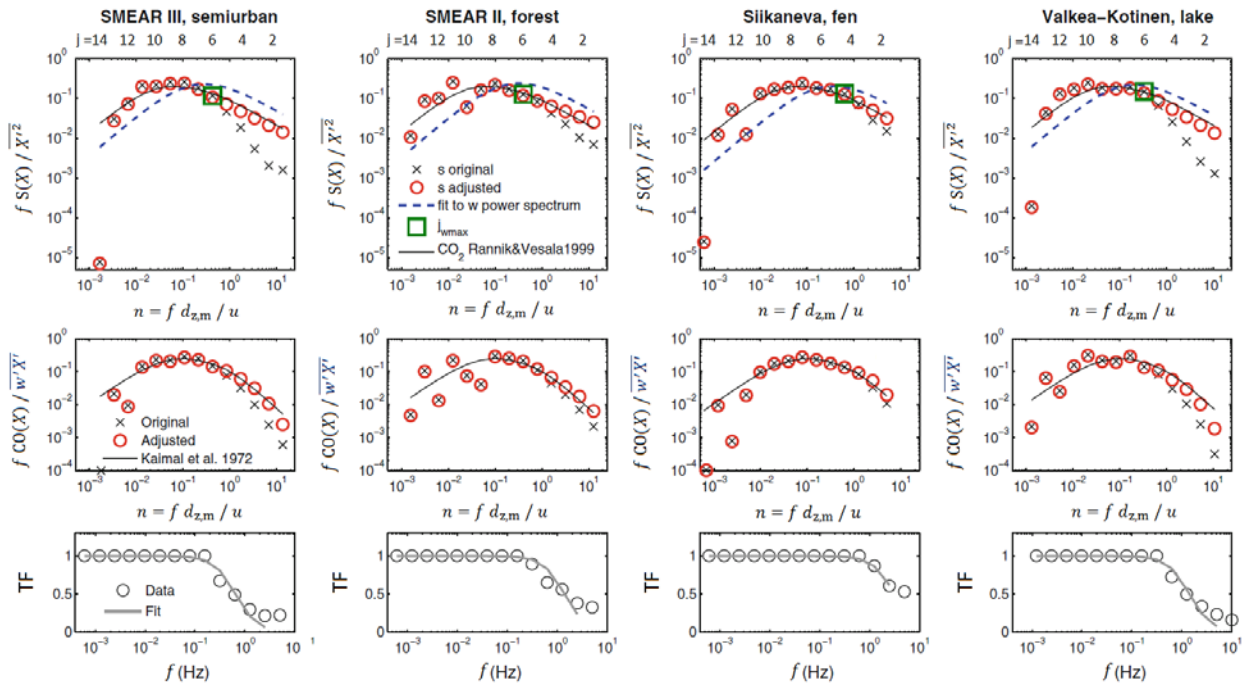


**Figure 2.** Modified after Nordbo and Katul (2012): Overview of the wavelet-based spectral correction method for four case studies. Top row: power spectra as function of the normalized frequency  $n$  (original with black crosses; adjusted with red circles). A fit to the power spectrum of  $w$  (blue dashed line) is used to derive the frequency limit  $n_{\max}(S(w))$  (green square). Atop the plot the scale indices  $j$  of the data points are displayed. Middle row: cospectra as a function of  $n$  (original with black crosses; adjusted with red circles) and the reference cospectrum of Kaimal et al. (1972) for comparison. Bottom row: deduced transfer function (TF) as a function of the natural frequency  $f$ .

(v) In Sect. 4.2.6 the required amplitude adjustment is performed for the selected wavelet coefficients of  $X$ ;

(iv) In Sect. 4.2.7 the corrected scalar time series is reconstructed from the unmodified and adjusted wavelet coefficients in the frequency ranges  $n(S(X)) \leq n_{\max}(S(w))$  and  $n(S(X)) > n_{\max}(S(w))$ , respectively. This is achieved by an inverse wavelet transform.

#### 4.2.2 Discrete wavelet transform

In wavelet analysis, a time series is decomposed into a set of small pulses of a predefined shape. Unlike Fourier transforms, wavelet transforms do not only retain the scale (inverse proportional to frequency) and amplitude information of a pulse, but also its location in time. Here a discrete wavelet transform is used, with an orthonormal wavelet basis and dyadically (powers of two) arranged scales. Details on the reasoning of this choice are provided by NK12, who define the discrete wavelet convolution as;

|   |                    |                  |
|---|--------------------|------------------|
| Title: NEON Algorithm Theoretical Basis Document – Frequency Response Corrections | Author: S. Metzger | Date: 08/02/2013 |
| NEON.DOC.000854   |                    | Revision: A      |

$$W_j[i] = \sum_{t=1}^{2^{J-j}} g_j[i - 2^j t] Y[t], \quad (3)$$

where  $W_j[i]$  is the wavelet coefficient (amplitude of variation) at scale index  $j \in \{1 \dots J\}$  and location index  $i \in \{1 \dots 2^{J-j}\}$ ,  $g_j$  is a discrete wavelet, and  $Y[t]$  is the time series of  $Y \in \{X, w\}$ , with the time position index  $t$ . In other words, if we have an EC raw data record of length  $2^{15} = 32768$ , then  $J = 15$  different eddy sizes are resolved, each described by the unique scale index  $j$ . The number of wavelet coefficients for each scale index  $j$  is expressed by  $2^{J-j}$ , ranging from  $2^{15-15} = 2^0 = 1$  for the largest scale to  $2^{15-1} = 2^{14}$  for the smallest scale, with an overall number of  $2^J - 1$  wavelet coefficients. Figure 3 shows a schematic illustration of the resulting scale vs. location representation of  $Y$  in the wavelet half-plane.

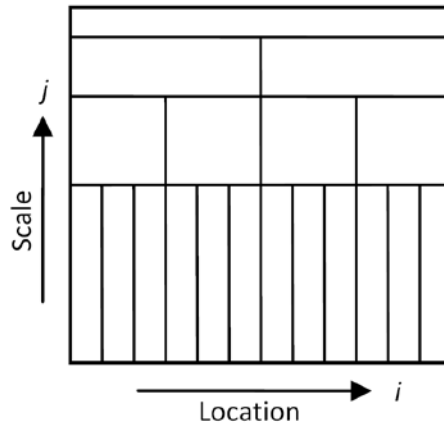


**Figure 3.** Relation of the resolution of location (index  $i$ ) and scale (index  $j$ ) for the discrete wavelet transform.

NK12 select the Haar Wavelet for the forward and backward transforms;

$$g(t) \begin{cases} 1 & 0 \leq t \leq 1/2 \\ -1 & 1/2 \leq t \leq 1 \\ 0 & \text{otherwise} . \end{cases} \quad (4)$$

In the wavelet transform,  $g$  is dilated (i.e. stretched) to match a scale of variation, and translated to correspond to a time location in  $Y$ . The variation frequency  $f_j$  and the normalized variation frequency  $n_j$  can be calculated for each scale index  $j$  as;

$$f_j = \frac{2^{J-j}}{2^J} f, \quad (5)$$

$$n_j = \frac{d_{z,m}}{\bar{u}} f_j, \quad (6)$$

with sampling frequency  $f$ , measurement height  $d_{z,m}$  and the average along-wind speed for a given averaging period  $\bar{u}$ . The wavelet variance  $\overline{Y'^2}$  (overbars and primes denote averages and immediate deviations from the average, respectively) is the mean of the squared wavelet coefficients over all scale and location indices;

$$\overline{Y'^2} = \frac{1}{2^J} \sum_{j=1}^J \sum_{i=1}^{2^{J-j}} (W_j[i])^2. \quad (7)$$

The NK12 spectral correction method commences by computing the normalized wavelet power spectrum  $S_n(Y)$  with  $Y \in \{X, w\}$ ;

$$S_{n,j}(Y) = f \frac{S_j(Y)}{Y'^2} = \frac{f_j}{f} \frac{\overline{W_j^2}}{Y'^2 \ln(2)} = \frac{2^{J-j}}{2^J} \frac{\overline{W_j^2}}{Y'^2 \ln(2)}, \quad (8)$$

with the function of the natural logarithm  $\ln()$ . The normalized wavelet power spectrum before correction and its scale indices are shown in Figure 2 (black crosses, NK12). For more information on wavelet analysis, NK12 provide a comprehensive reference list.

#### 4.2.3 Spectral peaks

A 100-point fit to the power spectrum (blue dashed line in Figure 2, top row) is used to determine the frequency  $j_{\max}(w)$  at which the peak in  $S_n(w)$  occurs (green square in Figure 2, top row). The Wavelet coefficients  $W_j(X)$  for which  $j < j_{\max}(w)$  are assumed to potentially require adjustment for high frequency spectral loss (e.g., scale indices 5–1 in Figure 2, top row, SMEAR III, NK12).

#### 4.2.4 Power law coefficient in the inertial subrange

The Wavelet coefficients  $W_j(X)$  for which scale index  $j_{\max}(w)-2 \leq j \leq j_{\max}(w)$  are used to determine how much  $W_j(X)$  at smaller scale indices ( $j < j_{\max}(w)$ ) are to be adjusted (e.g., scale indices 6–8 in Figure 2, top row, SMEAR III). Obtaining the ISR power law coefficient from scale indices  $j_{\max}(w)-2 \leq j \leq j_{\max}(w)$  is based on the argument that e.g. tube effects do not attenuate the lower frequencies residing in the ISR. The un-attenuated log–log scale slope (power law coefficient) in the inertial subrange of  $S(X)$  is obtained from least-squares regression over  $S_j(X)$  for scale indices  $j_{\max}(w)-2 \leq j \leq j_{\max}(w)$ . If the regression slope falls within  $-1.8 \dots -1.3$  it will be deemed as plausible and used for extrapolation to obtain the un-attenuated power at smaller scale indices ( $j < j_{\max}(w)$ ). The bounds  $-1.8 \dots -1.3$  are conservatively chosen to accommodate effects such as intermittency or wakes that may cause anomalous departures from the  $-5/3$  law of isotropic turbulence in the ISR. If the departure however exceeds the bounds  $-1.8 \dots -1.3$ , the conventional  $-5/3$  slope is used as a logical alternative (NK12).

#### 4.2.5 Distribution of amplitude adjustment

In the theoretical and the experimental approaches, high-frequency attenuation is compensated by adjusting the cospectral energy for each averaging interval, irrespective of within-averaging interval variations. In reality however, e.g. tube wall effects do not only attenuate the amplitude of a signal, but also distort (or smear) its travel-time. In the Wavelet half-plane, travel-time distortions show as smeared spectral energy along the locations of the wavelet coefficients, and can be addressed explicitly. That is, some spectral energy is attributed to wavelet coefficients that should not have energy, and thus should also not be amplified. To compensate this distortion, only those scalar wavelet coefficients  $W_j(X)[i]$  are adjusted for which the corresponding wavelet coefficients of the vertical wind  $W_j(w)[i]$  are sufficiently energetic. The criterion used here is that  $(W_j(w)[i])^2$  has to be among the largest coefficients that contribute to 90% of the local scale-wise total energy. That is, for each scale index  $j < j_{\max}(w)$  for which  $W_j(X)$  needs to be adjusted, a subgroup of position indices  $i_c$  is selected for correction, and another subgroup of position indices  $i_o$  remains unaltered (NK12).

#### 4.2.6 Correction for high-frequency loss

Now that the scale and position indices of the wavelet coefficients to be adjusted are known, the amplitude adjustment can be made. (i) the corrected amplitudes  $A_{j,c}(X) = \sqrt{S_{j,c}(X)}$  are calculated for each scale in the potentially attenuated range of scale indices  $j < j_{\max}(w)$ . This is achieved by extrapolating the ISR log-log scale slope (determined in Sect. 4.2.4) into the range of scale indices  $j < j_{\max}(w)$ , resulting in  $S_{j,c}(X)$ . (ii) The dimensionless amplification energy in each scale  $E_j$  is found from the ratio between the un-attenuated amplitudes and the attenuated amplitudes. A weighting procedure is used to take into account that only a selected fraction of all wavelet coefficients for a given scale are adjusted;

$$E_j = \left( \frac{A_{j,c}}{A_j} \right)^2 \frac{\overline{W_j^2[t_c, t_0]} N(i_c, t_0) - \overline{W_j^2[t_0]} N(i_o)}{\overline{W_j^2[t_c]} N(i_c)}, \quad (9)$$

with  $N(i_o)$  and  $N(i_c)$  being the number of wavelet coefficients that remain unaltered and those that are selected for correction, respectively, and  $N(i_o, i_c) = N(i_o) + N(i_c)$ . The fraction  $A_{j,c}/A_j$  is not allowed to be below unity, i.e. the correction cannot dampen wavelet coefficients. The corrected wavelet coefficients are then given as;

$$W_{j,c}[i_c] = W_j[i_c] \sqrt{E_j}. \quad (10)$$

Thus, the amplitude adjustment is completely based on the time-localization feature of wavelets, though  $E_j$  stays the same for a certain scale (NK12).

|   |                    |                  |
|---|--------------------|------------------|
| Title: NEON Algorithm Theoretical Basis Document – Frequency Response Corrections | Author: S. Metzger | Date: 08/02/2013 |
| NEON.DOC.000854   |                    | Revision: A      |

#### 4.2.7 Reconstruction of the corrected time series

Lastly, the corrected time series of  $X$ ,  $X_c$ , is reconstructed by performing an inverse wavelet transform over unadjusted  $W_j(X)$  at larger scale indices ( $j \geq j_{\max}(w)$ ) and adjusted  $W_{j,c}(X)$  at smaller scale indices ( $j < j_{\max}(w)$ ).

### 5 ALGORITHM IMPLEMENTATION

The implementation of Eqs. (3)–(10) is organized in three steps, which also include the consideration of previously determined data quality flags and metrics (AD[03]);

(i) If more than 10% of the observations of either  $w$  or  $X$  are rendered unsuitable (respective quality metric  $QM_{\text{hard}} > 10\%$ ), no correction is performed, and the algorithm stops here (Mauder and Foken, 2011).  $X$  is assigned to  $X_c$ , and the corresponding averaging period is assigned a quality metric  $QM_{\text{att}} = 100\%$ , indicating that no correction for spectral loss could be performed.

(ii) If  $QM_{\text{hard}} \leq 10\%$  for both  $w$  and  $X$ , shift  $X$  by  $l_x$  with respect to  $w$  to offset the decorrelation effect of along-wind sensor separation. Discard observations of  $w$  and  $X$  with respective quality flag  $QF_{\text{hard}} = 1$ . Perform a linear interpolation over the time series of  $w$  and  $X$  to fill the missing values. This procedure solely facilitates correcting high-frequency spectral loss for all suitable observations (respective quality flag  $QF_{\text{hard}} = 0$ ). For this purpose continuous data sets of  $w$  and  $X$  with all artifacts removed are required. However, the interpolated data points are not used for the calculation of means, variances or covariances from EC-TES variables (AD[03]).

(iii) De-trend both  $w$  and  $X$ , and perform Eqs. (3)–(10) as implemented in detail for a test dataset in the NK12 source code (AD[08]). Assign a quality metric  $QM_{\text{att}} = 0\%$  to the corresponding averaging period.

$X_c$  and  $QM_{\text{att}}$  shall be reported as results of this ATBD, i.e. they shall be made available as input variables for subsequent ATBDs (Table 1).

### 6 UNCERTAINTY

This section concerns only the propagation of sensor/calibration uncertainty in the input variables, through the presented algorithms, into the variables reported in this ATBD. This section does not concern testing the fulfillment of assumptions in the EC method, quantification of sampling errors and the like. These sources of uncertainty are addressed in a series of tests during the implementation of AD[01] (details provided therein).

Once all higher-level NEON DPs are mapped out, an integrated uncertainty propagation plan will be derived. At the present time this section represents a simplified indicator for the potential direction of

such uncertainty propagation plan. For this purpose resolution is defined as the smallest detectable change in a variable, and accuracy and precision are defined as the systematic and random uncertainties in a variable, respectively. In the following sections, generic algorithms are provided that enable the propagation of resolution, accuracy and precision through Eqs. (3)–(10).

## 6.1 Analysis of uncertainty

Following Taylor (1997) the maximum probable error  $\sigma_A$  of a function  $F$  with  $N$  input variables ( $X$ ) is defined as;

$$\sigma_A(F) = \sum_{i=1}^N \left| \frac{\partial F}{\partial X_i} \right| \sigma_A(X_i). \quad (11)$$

The partial derivative  $\partial F/\partial X_i$  is the slope of  $F$  with  $X_i$ , and hence quantifies the sensitivity of  $F$  on uncertainty in  $X_i$ . In the following, Eq. (11) is used as model for the propagation of accuracy (subscript A) through Eqs. (3)–(10). If random and independent, the uncertainties in  $X_i$  tend to cancel, and Gaussian quadrature applies;

$$\sigma_P^2(F) = \sum_{i=1}^N \left( \frac{\partial F}{\partial X_i} \sigma_P(X_i) \right)^2. \quad (12)$$

Eq. (12) is used as the model for the propagation of precision (subscript P) and resolution through Eqs. (3)–(10). At this point, it is assumed that the resolution follows a binomial distribution (low amplitude noise between two adjacent discrete values, Vickers and Mahrt, 1997). For sufficiently large sample sizes (20 or greater, Box et al., 2005), the binomial distribution is reasonably approximated by the normal distribution, and can be quantified by Gaussian metrics such as Eq. (12).

## 6.2 Reported uncertainty

In order to calculate the accuracy, precision and resolution for each reported variable in Table 1, the partial derivatives of Eqs. (3)–(10) shall be found, and combined in accordance with Eqs. (11)–(12). Eq. (12) analogously applies for the determination of the resulting resolution, when replacing the precisions (standard deviations)  $\sigma_P$  with the resolutions (finite differences)  $\Delta_R$ .

## 7 ALGORITHM VERIFICATION

Verification of the algorithms disclosed in this ATBD shall follow the procedures outlined in AD[09]. During the implementation of AD[01], DPs will be derived from the present algorithms, and DP verification and validation will be specified accordingly.

|   |                           |                         |
|---|---------------------------|-------------------------|
| <i>Title:</i> NEON Algorithm Theoretical Basis Document –<br>Frequency Response Corrections | <i>Author:</i> S. Metzger | <i>Date:</i> 08/02/2013 |
| NEON.DOC.000854   |                           | <i>Revision:</i> A      |

## 8 SCIENTIFIC AND EDUCATIONAL APPLICATIONS

The correction of high-frequency spectral loss is the basis to confidently process EC turbulence data into higher-level DPs with ecological relevance. The present ATBD details all relevant transformations as well as the propagation of uncertainty through these transformations. During the implementation of AD[01], data will continue to be processed into higher-level DPs. Ecologically relevant high-level DPs of the EC-TES include the exchange of heat, water vapor and CO<sub>2</sub> between the land surface and the atmosphere. These DPs are used for constraining, calibrating and validating process-based models (e.g., Rastetter et al., 2010). This shall enable the detection of continental scale ecological change and the forecasting of its impacts.

Standardized and transparent documentation intends to foster reproducibility of all data processing steps. For this purpose, it is planned to make all processing steps available as open-source code in a high-level programming language. Aside from enabling direct feedback from the research community, this also provides community members (e.g. students at graduate level) a straightforward and hands-on toolbox for data processing of micrometeorological measurements.

## 9 FUTURE PLANS AND MODIFICATIONS

This ATBD will be version controlled, i.e. future developments might result in modifications to this ATBD, which will be documented accordingly.

## 10 APPENDIX

### 10.1 Acronyms

| Acronym         | Description                                     |
|-----------------|---|
| ATBD            | Algorithm theoretical basis document            |
| C <sup>3</sup>  | Command, control, and configuration document    |
| CO <sub>2</sub> | Carbon dioxide                                  |
| DP              | Data product                                    |
| EC              | Eddy covariance                                 |
| EC-TES          | Eddy-covariance turbulent exchange subsystem    |
| FFT             | Fast Fourier transform                          |
| FIU             | Fundamental instrument unit (NEON project team) |

| Acronym          | Description  |
|------------------|--|
| H <sub>2</sub> O | Water vapor  |
| IRGA             | Infrared gas analyzer  |
| NEON             | National Ecological Observatory Network  |
| NK12             | Nordbo, A. & Katul, G. (2012) A wavelet-based correction method for eddy-covariance high-frequency losses in scalar concentration measurements. <i>Boundary-Layer Meteorology</i> , <b>146</b> , 81-102. |
| QA/QC            | Quality Assurance/Quality Control  |

## 10.2 Functions

| Function                           | Description   |
|------------------------------------|---|
| []                                 | Position index  |
| CO                                 | Cospectrum  |
| $\partial$                         | Partial differential operator   |
| $\Delta$                           | Finite difference operator  |
| $\in\{X, Y\}$                      | Element of a set that includes $X$ and $Y$  |
| F                                  | Function for error propagation  |
| ln                                 | Natural logarithm   |
| S                                  | Power spectrum  |
| $\sigma$                           | Standard deviation  |
| TF                                 | Transfer function   |
| $\bar{X}$                          | Short-term (e.g., 30 min) arithmetic mean of atmospheric quantity $X$             |
| $\overline{X'X'}, \overline{X'^2}$ | Short-term (e.g., 30 min) sample variance of atmospheric quantity $X$             |
| $\overline{X'Y'}$                  | Short-term (e.g., 30 min) sample covariance of atmospheric quantities $X$ and $Y$ |

### 10.3 Parameters

| Parameter | Description | Numeric value | Units                    |
|-----------|-------------|---------------|--------------------------|
| $J$       | Sample size | User-defined  | Dimensionless<br>(count) |
| $N$       | Sample size | User-defined  | Dimensionless<br>(count) |

### 10.4 Subscripts

| Subscript | Description  |
|-----------|--|
| 1... $N$  | Numeric identifier   |
| A         | Accuracy   |
| c         | Corrected  |
| hard      | Measurement or instrument conditions that do not permit data usage |
| i         | Running index  |
| j         | Running index  |
| m         | Measurement  |
| max       | Maximum  |
| n         | Normalized   |
| P         | Precision  |
| R         | Resolution   |
| X, Y      | Placeholder for atmospheric quantities                             |
| x, y, z   | Along-, cross- and vertical axes of a Cartesian coordinate system  |

## 10.5 Variables

| Variable     | Description   | Units                                     |
|--------------|---|---|
| $A$          | Amplitude   | Depending on use case                     |
| $d$          | Distance/length/height  | m   |
| $d_{x,FP90}$ | Cross-wind integrated upwind extent from within which 90% of an observed value is sourced | m   |
| $d_{z,d}$    | Displacement height   | m   |
| $E$          | Energy  | Depending on use case                     |
| $f$          | Frequency   | Hz  |
| $F$          | Flux into or out of an ecosystem  | Depending on unit of scalar               |
| $i$          | Running index   | Dimensionless (count)                     |
| $j$          | Running index   | Dimensionless (count)                     |
| $l$          | Lag time  | s   |
| $n$          | Normalized frequency  | Dimensionless                             |
| $QF$         | Quality flag  | Dimensionless (0 or 1)                    |
| $QM$         | Quality metric (same subscripts as for QF apply)  | %   |
| $t$          | Time  | s   |
| $u, v, w$    | Along-, cross- and vertical wind speed  | $m\ s^{-1}$                               |
| $x, y, z$    | Along-, cross- and vertical axes of a Cartesian coordinate system                         | Dimensionless                             |
| $X, Y$       | Placeholder for atmospheric quantities  | Depending on unit of atmospheric quantity |

## 11 BIBLIOGRAPHY

Box, G. E. P., Hunter, J. S. & Hunter, W. G. (2005) *Statistics for experimenters: design, innovation, and discovery*. John Wiley & Sons, New York, Chichester, Brisbane, Toronto, Singapore.

De Ligne, A., Heinesch, B. & Aubinet, M. (2010) New Transfer Functions for Correcting Turbulent Water Vapour Fluxes. *Boundary-Layer Meteorology*, 137, 205-221.

Foken, T. (2008) *Micrometeorology*. Springer, Berlin, Heidelberg.

Foken, T., Leuning, R., Oncley, S. P., Mauder, M. & Aubinet, M. (2012) Corrections and data quality control. *Eddy covariance: A practical guide to measurement and data analysis* (eds M. Aubinet, T. Vesala & D. Papale), pp. 85-131. Springer, Dordrecht, Heidelberg, London, New York.

Fratini, G., Ibrom, A., Arriga, N., Burba, G. & Papale, D. (2012) Relative humidity effects on water vapour fluxes measured with closed-path eddy-covariance systems with short sampling lines. *Agricultural and Forest Meteorology*, 165, 53-63.

Horst, T. W. & Lenschow, D. H. (2009) Attenuation of scalar fluxes measured with spatially-displaced sensors. *Boundary-Layer Meteorology*, 130, 275-300.

Kaimal, J. C. & Finnigan, J. J. (1994) *Atmospheric boundary layer flows: Their structure and measurement*. Oxford University Press, New York.

Kaimal, J. C., Wyngaard, J. C., Izumi, Y. & Coté, O. R. (1972) Spectral characteristics of surface-layer turbulence. *Quarterly Journal of the Royal Meteorological Society*, 98, 563-589.

Loescher, H. W., Law, B. E., Mahrt, L., Hollinger, D. Y., Campbell, J. & Wofsy, S. C. (2006) Uncertainties in, and interpretation of, carbon flux estimates using the eddy covariance technique. *Journal of Geophysical Research, [Atmospheres]*, 111, D21S90-.

Mauder, M. & Foken, T. (2011) Documentation and Instruction Manual of the Eddy-Covariance Software Package TK3. pp. 60. Universität Bayreuth, Abteilung Mikrometeorologie, Bayreuth.

Moore, C. J. (1986) Frequency-Response Corrections For Eddy-Correlation Systems. *Boundary-Layer Meteorology*, 37, 17-35.

Nordbo, A. & Katul, G. (2012) A wavelet-based correction method for eddy-covariance high-frequency losses in scalar concentration measurements. *Boundary-Layer Meteorology*, 146, 81-102.

Rastetter, E. B., Williams, M., Griffin, K. L., Kwiatkowski, B. L., Tomasky, G., Potosnak, M. J., Stoy, P. C., Shaver, G. R., Stieglitz, M., Hobbie, J. E. & Kling, G. W. (2010) Processing arctic eddy-flux data using a

|   |                    |                  |
|---|--------------------|------------------|
| Title: NEON Algorithm Theoretical Basis Document – Frequency Response Corrections | Author: S. Metzger | Date: 08/02/2013 |
| NEON.DOC.000854   |                    | Revision: A      |

simple carbon-exchange model embedded in the ensemble Kalman filter. *Ecological Applications*, 20, 1285-1301.

Runkle, B., Wille, C., Gažovič, M. & Kutzbach, L. (2012) Attenuation Correction Procedures for Water Vapour Fluxes from Closed-Path Eddy-Covariance Systems. *Boundary-Layer Meteorology*, 142, 401-423.

Ruppert, J., Thomas, C. & Foken, T. (2006) Scalar similarity for relaxed eddy accumulation methods. *Boundary-Layer Meteorology*, 120, 39-63.

Schmid, H. P. (1994) Source areas for scalars and scalar fluxes. *Boundary-Layer Meteorology*, 67, 293-318.

Spank, U. & Bernhofer, C. (2008) Another Simple Method of Spectral Correction to Obtain Robust Eddy-Covariance Results. *Boundary-Layer Meteorology*, 128, 403-422.

Stull, R. B. (1988) *An Introduction to Boundary Layer Meteorology*. Kluwer Academic Publishers, Dordrecht.

Taylor, J. R. (1997) *An Introduction to Error Analysis: The Study of Uncertainties in Physical Measurements*. University Science Books, Mill Valley, California.

Vesala, T., Kljun, N., Rannik, U., Rinne, J., Sogachev, A., Markkanen, T., Sabelfeld, K., Foken, T. & Leclerc, M. Y. (2008) Flux and concentration footprint modelling: State of the art. *Environmental Pollution*, 152, 653-666.

Vickers, D. & Mahrt, L. (1997) Quality control and flux sampling problems for tower and aircraft data. *Journal of Atmospheric and Oceanic Technology*, 14, 512-526.